513 Mbit/s Visible Light Communications Link Based on DMT-Modulation of a White LED

Jelena Vučić, Christoph Kottke, Stefan Nerreter, Klaus-Dieter Langer, and Joachim W. Walewski

***Abstract*—We report a visible-light wireless point-to-point communication link operating at 513 Mbit/s gross transmission rate (net ∼450 Mbit/s). The bit-error ratio of the uncoded data was smaller than $2 \cdot 10^{-3}$ for an illumination level of ∼1000 lx. The link was based on a commercial thin-film high-power phosphorescent white LED, an avalanche photo diode, and off-line signal processing of discrete multitone signals. Quadrature-amplitude modulation, bit- and power-loading, as well as symmetrical clipping were successfully employed in pushing the gross transmission rate beyond 500 Mbit/s. Adaptation of the clipping level increased the data rate only by 2%, while simulations predicted an enhancement of 20%. Obstacles towards higher data rates as well as potential remedies are discussed. We predicted that data rates of over 1 Gbit/s can be achieved with the same setup and under the same experimental conditions if these obstacles are overcome.**

***Index Terms*—Bit- and power-loading, clipping level adaption, discrete multitone, optical-wireless communications, visible-light communications, white phosphorescent LED.**

I. Introduction

HIGH-POWER white light-emitting diodes (LEDs) are an emerging technology for energy-efficient artificial lighting. Besides appealing lighting properties, like the ease of colour rendering, the potential synergy of illumination and data transmission functions by use of one optical source has stimulated worldwide research and development activities [1] as well as global standardization efforts [2]. Visible-light communications (VLC) technology has many attractive assets, such as worldwide available and unlicensed bandwidth, non-interference with radio bands, and the potential of spatial reuse of operating frequencies in adjacent communication cells. VLC may offer an additional service at comparably low extra cost due to the future ubiquitous LED lighting and signaling infrastructure. An overview of the technical constraints and challenges for VLC links can be found elsewhere [1].

Concerning the practical data rates achievable with such wireless links, Vucic *et al.* recently demonstrated 230 Mbit/s gross with a single white LED luminary and a low-cost PIN diode [3]. The modulation format used was quadrature-amplitude-modulation (QAM) on discrete multitones (DMT). Later, utilizing an LED module featuring 30% larger bandwidth than that in [3] and an avalanche photodiode (APD) in the receiver, the same group demonstrated a similar transmission rate with on-off keying (OOK), [4]. In both cases, the data rate was ultimately limited by the bandwidth of the transmitter and the intrinsic noise in the receiver.

In this publication, we demonstrate that (1) by use of low-noise photo detection in the quantum-noise limit (due to the employed APD), and (2) by efficiently exploiting the modulation bandwidth and high SNR of the used LED emission (the same module as in [4]) due to the employed DMT with quadrature-amplitude modulation, bit- and power-loading, as well as symmetrical clipping, the achievable data rate can be increased more than twice to reach 513 Mbit/s gross. We discuss impediments towards further data rate enhancements and provide simulation-based predictions for data rates feasible in the presented practical system if these impediments can be overcome (1.14 Gbit/s gross). Moreover, we calculate the corresponding theoretical capacity upper bound based on water-filling (1.74 Gbit/s). It is worth mentioning that our work does not aim not at improving the DMT modulation and its powerful adaption to dispersive power-limited channels, but at applying these techniques to a new field of research and development, i.e., VLC. Thanks to these techniques and a deeper understanding of high-power white LEDs, we have continuously improved the data rate achievable with phosphorescent LEDs [3], [5].

II. Experimental Setup

We first performed a measurement of the electro-optical-electrical (EOE) channel frequency response, followed by the measurements of DMT-based transmission performance. The experimental setups are shown in Fig. 1, with dashed lines denoting the components involved in the channel-response measurement.

At the analogue Tx front-end (Tx in Fig. 1), the input signal (coming either from a function generator, or an arbitrary-waveform generator) was first amplified (Mini Circuits ZHL-6A) with the purpose to increase the LED modulation depth for the transmission experiment and then superimposed onto the LED bias current by aid of a bias T (Aeroflex 8810). Its output was directly supplied to the LED module without impedance matching. The light source was a commercial phosphorescent

Manuscript received July 15, 2010; revised September 17, 2010; accepted October 17, 2010. Date of publication October 25, 2010; date of current version December 03, 2010. This work was supported in part by European Commission's Seventh Framework Programme FP7/2007-2013 under Grant 213311, also referred to as OMEGA. The authors acknowledge the contributions of OMEGA colleagues. This information reflects the consortiums view, and the Commission is not liable for any use that may be made of any of the information contained therein.

J. Vučić, C. Kottke, and K.-D. Langer are with the Fraunhofer Institute for Telecommunications, Heinrich Hertz Institute, 10587 Berlin, Germany (e-mail: jelena.vucic@hhi.fraunhofer.de).

S. Nerreter is with Siemens AG, Corporate Technology, 13629 Berlin, Germany.

J. W. Walewski is with Siemens AG, Corporate Technology, Communication Technologies, 81739 Munich, Germany

Color versions of one or more of the figures in this paper are available online at http://ieeexplore.ieee.org.

Digital Object Identifier 10.1109/JLT.2010.2089602

0733-8724/$26.00 © 2010 IEEE

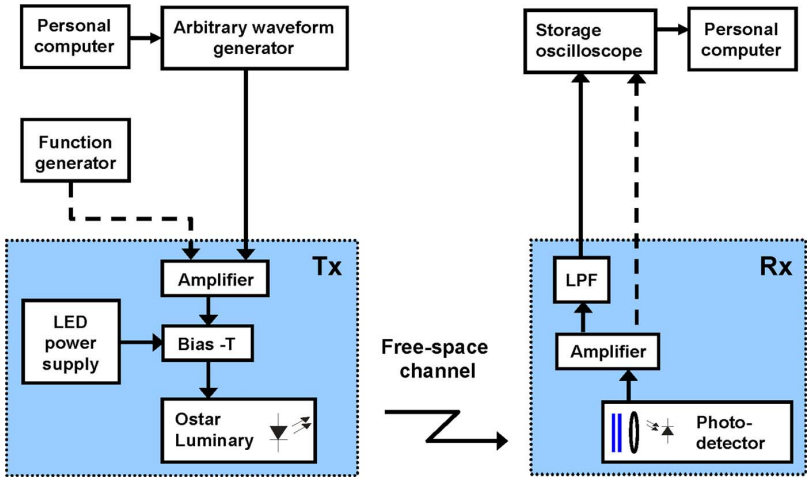

Fig. 1. Experimental setup. Dashed lines denote the setup used for measurement of the EOE channel frequency response. LPF: Low-pass filter.

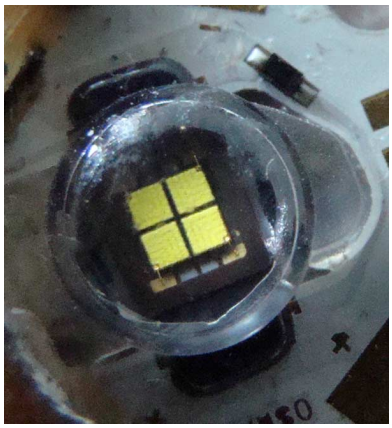

Fig. 2. Photograph of the commercial LED luminary (with spherical lens), as used in the measurements.

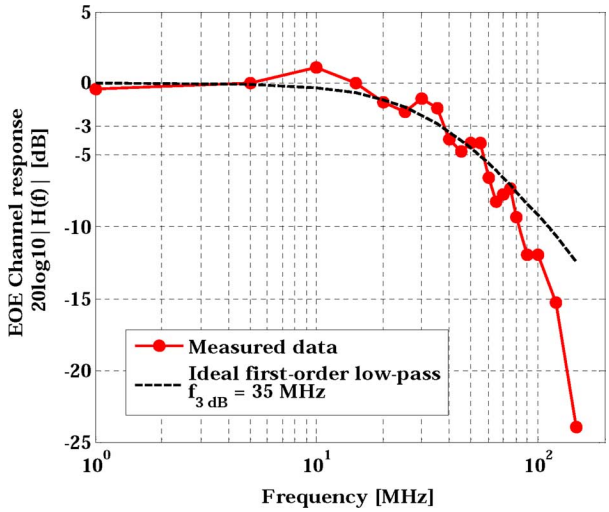

Fig. 3. EOE channel response of the data-transmission link in Fig. 1.

white LED module (OSTAR® LE CW E2B, see Fig. 2), devised for lighting applications. This module consists of four chips, providing a luminous flux of ∼250 lm (at 700 mA dc). This module comes with a factory-designed spherical lens, converting the emission from the rectangular LED module into a divergent light beam with a 130° full opening angle at 50% maximum intensity.

All experiments were performed at a certain brightness level (illuminance) in front of the receiver. Illuminance values of around 1000 lx were chosen in agreement with the lighting standard for well-lit working environments [6] and realized by separating the Tx and Rx module by an appropriate distance. Brightness levels were checked by a light meter placed at the position of the receiver in the otherwise dark laboratory. Deployment of a single module resulted in a relatively short link length (∼0.3 m for 1000 lx). Nevertheless, given that the used source is primarily devised for lighting purposes, we considered the illuminance at the receiver as the most relevant design parameter, [7]. In practical indoor scenarios with wireless distances of several meters the specified brightness levels needed for illumination can be achieved by using several LED modules and/or stronger collimation of the emitted light beam.

The ac-coupled analogue receiver (Rx in Fig. 1) consisted of the following components. An optical short-pass filter (customized design from Berliner Glas) with a cut-off wavelength of 500 nm was mounted in front of the photodiode to suppress the phosphorescent component of the LED radiation. A commercial large-area silicon APD (Electro Optics, C30872, 3 mm diameter) combined with an aspherical glass lens (New Focus 5728-A, 0.5 NA and 8 mm focal length) was used for detection. An amplifier (Pico-Amps pA4-00125-76) boosted the signal level up to the operation range of the storage oscilloscope (Agilent MSO71041, 4 GS/s sampling rate). Finally, the output amplitude was either directly monitored with the oscilloscope or stored for off-line demodulation.

The magnitude of the channel's frequency response was measured by varying the frequency of a small-signal sine wave provided by the function generator, and directly monitoring the receive amplitude at the oscilloscope. Fig. 3 presents the measured magnitude of the EOE channel frequency response. Since the receiver itself has a relatively large bandwidth (APD ∼80 MHz, amplifier ∼2.3 GHz), it can be concluded from the figure that the system bandwidth (∼35 MHz) is limited by the LED module.

For transmission-performance measurements, time traces of a DMT signal were generated by software and fed to the arbitrary-waveform generator (Tektronix AWG5012). The real-valued DMT signal consisted of $N-1=127$ modulated subcarriers within a bandwidth of $B=100$ MHz in the baseband ($B/N=0.781$ MHz subcarrier spacing, no zero-padding).[1] The input to the inverse fast Fourier transform corresponding to dc was left unmodulated.

Modulation beyond the 3-dB channel bandwidth, as well as the presence of radio interference in our laboratory (due to only partially shielded hardware) significantly enhanced the noise at some frequencies. For this reason, bit- and power-loading (i.e., use of flexible constellation sizes of the subcarriers) were applied to the subcarriers, with the orders of the QAM constellations adapted to the channel quality at individual frequencies. As a result, the transmission rate was enhanced while a similar bit-error ratio (BER) was retained over the whole transmission band. The next section provides a more detailed discussion of the exact modulation orders of individual subcarriers used in our experiments.

In the measurements, the DMT waveform (analogue signal at the AWG output) was scaled to the output range of the amplifier driving the LED (5.4 V peak-to-peak). The amplified ac signal was superimposed onto the 100 mA dc bias current, which resulted in an LED modulation index of $\sim$16%.

The received electrical signal was passed through a high-order low-pass antialiasing filter with 100 MHz cut-off frequency, after which the time traces were recorded with the real-time storage oscilloscope (at 4 GS/s sampling rate) and further processed off-line. The received DMT signal was downsampled, demodulated, and signals on the subcarriers were separately de-mapped according to the applied bit-loading mask. Perfect synchronization between transmitter and receiver was realized (the start of the transmission frame was manually adjusted). By use of a training sequence, the channel was estimated, and the estimates were used for data equalization. In the experiments, the training sequence consisted of 10 DMT symbols sent at the beginning of the transmission block, which was sufficient for high-fidelity channel estimates. BERs were calculated for each modulated subcarrier. The DMT data sequences (including training symbols), were chosen sufficiently long to collect more than 20 symbol errors on each modulated subcarrier.

In contrast to the channel response measurements, all data-transmission experiments were performed in the presence of sunlight flooding through the laboratory windows and lit fluorescent ceiling lighting.

III. Results and Discussion

As previously mentioned, we resorted to bit- and power-loading in order to efficiently exploit the channel capacity. Based on the knowledge of the EOE channel, a loading algorithm determines the QAM order and power of individual subcarriers, leading to a maximized aggregate transmission rate. Hereby, the algorithm complies with the constraint on the overall power of the DMT signal and on the maximum acceptable BER (on each subcarrier) as specified for a given system [8].

In this work, we applied an optimal and fast-converging loading algorithm proposed by Krongold *et al.* [9], developed for application in DSL systems, considering binary phase shift-keying (BPSK) and QAM for symbol mapping. It uses the Lagrange multiplier method to maximize the discrete function of the total system throughput (i.e., spectral efficiency) under the total signal power constraint

$$\max\left(\sum_{n=1}^{N-1} R_n\right) \quad \text{for} \quad \sum_{n=1}^{N-1} P_n \le P_{\max} \tag{1}$$

where $N-1$ denotes the number of subcarriers (carrying information) in the system, $R_n=\log_2 M_n$ represents the (integer) number of bits allocated to the nth subcarrier, e.g., via an M-QAM modulation, and $P_n=\langle X_n^2\rangle$ represents the constellation power which is needed for symbol complexity R_n to be detected with a given BER. The signal power is limited by $P_{\max}$.

Beside the BER and signal power constraints, loading algorithm requires knowledge of channel-state information. The channel state is represented in form of noise-enhancement coefficients $\sigma^2/|H_n|^2$ on subcarrier frequencies n, where σ^2 is the power of the additive white Gaussian noise (AWGN)[2] within the subcarrier bandwidth, and $|H_n|$ the corresponding channel-gain coefficient. Due to the limited space and in order to remain within the focus of our paper, the details of the loading algorithm used are not reviewed here. Exhaustive explanation of the algorithm steps can be found elsewhere in the literature [9].

The needed $\sigma^2/|H_n|^2$ coefficients were obtained after conducting an initial BER measurement. In this initial measurement we chose to modulate each subcarrier with equal power $P_n=\text{const.}$ for $n=1,\ldots,N-1$ and to manually set arbitrary subcarrier modulation orders M_n (M_n varied over subcarriers). Since BER is a monotonous function of the SNR for a certain M, from BER_n values obtained by the measurement, we calculated the SNR of the nth subcarrier by use of the analytical expressions valid for an AWGN channel [10]. The SNR on the nth subcarrier is given as

$$\text{SNR}_n=\frac{P_n}{\sigma^2/|H_n|^2}. \tag{2}$$

With so obtained SNRs, i.e., $\sigma^2/|H_n|^2$ coefficients[3], we were able to apply the loading algorithm and get an optimal bit and power distribution for the given channel and for the chosen BER. For the ultimate BER limit in our system we chose $2\cdot10^{-3}$, which can readily be suppressed to below 10^{-16} by use of forward-error correction algorithms [11]. However, we set the BER

[1]DMT parameters were chosen as good rule-of-thumb values for the system and VLC channel at hand; no optimization efforts in this sense were made.

[2]Depending on whether the preamplifier or the background light generate the dominant noise component, noise at the receiver can either be frequency dependent or white. In any case, we consider that the noise power can be regarded as constant within the subcarrier bandwidth.

[3]It is important to note that the signal total power $(N-1)P_n$ (here only the positive frequencies are regarded) can be arbitrarily chosen, as long as we use the same value to constrain the loading algorithm, since the algorithm results depend on the ratio $((N-1)P_n)/(\sigma_n^2/|H_n|^2)$.

limit of the loading algorithm to $1 \cdot 10^{-3}$ to allow a margin for the effects not accounted for by the loading algorithm decision (such as clipping).

In a measurement that was performed with the optimal distributions (resulting from the loading algorithm), we achieved a gross data rate

$$R = \frac{B}{N} \sum_{n=1}^{N-1} R_n \tag{3}$$

of 500 Mbit/s and an error performance $\mathrm{BER}_{\mathrm{TOT}} = 1.2 \cdot 10^{-3}$ (the number of falsely detected bits over the number of transmitted bits on all subcarriers). The gross rate does not include subtraction for redundancy of cyclic prefix and overhead needed for error correction coding or training, which can be estimated in total at 11% [3].

With the same loading mask and for the same channel conditions, we also performed Monte Carlo simulations (500 000 symbols per subcarrier), which predicted a $\mathrm{BER}_{\mathrm{TOT}}$ of $9.2 \cdot 10^{-4}$. Even though measurements resulted in a BER slightly over the targeted value, the result was acceptable, since it was still below the $2 \cdot 10^{-3}$ FEC limit.

If the goal is to stay within the mentioned FEC limit, one can try to increase the transmission rate even more by increasing the total signal power and allowing for some controlled clipping of the electrical signal [12]. Due to its subcarrier nature, a DMT signal waveform is plagued by occasionally-occurring large peaks in an otherwise rather low-power signal. If the signal amplitude at the LED input is adjusted so that the peaks of the DMT signal still lie within the LED operation range, the power of the transmitted data signal is on average very low. In order to improve the power efficiency, symmetrical clipping of the DMT signal in front of the LED has successfully been applied before [3].

We actually applied symmetric clipping to the digital signal at the Tx amplifier input, already in the measurements described here. However, in these measurements, we set a very conservative clipping level, since we wanted to evoke a quasi-no-clipping situation for these start trials.[4] Assuming that a DMT signal in time domain is approximately Gaussian in distribution with variance $\langle x^2 \rangle = 2 \sum_{n=1}^{N-1} \langle X_n^2 \rangle = 2P$ (due to conjugate symmetry, the negative frequencies also carry power P), we set the clipping limits to $|x_{\mathrm{C}}| = 4.5\sqrt{2P}$. This corresponded to a clipping level $\mathrm{CL} = 20 \log(|x_{\mathrm{C}}|/\langle x^2 \rangle)$ of about 13 dB. The same was done for simulations. In the experiment, the clipping limits were scaled to the output range of the pre-amplifier, i.e., 5.4 Vpp. Indication that the 13 dB clipping level (i.e., signal range) was sufficiently large to ensure practically no clipping occurrences was obtained from the fact that the simulations resulted in such BER values, which did not exceed the ones targeted by the loading algorithm, even though the algorithm does not take clipping effects into account.

[4]This was especially important for the initial BER measurement. Since the loading algorithm only takes into account the errors due to AWGN, but not due to clipping, clipping occurrences would result in false input values for the algorithm.

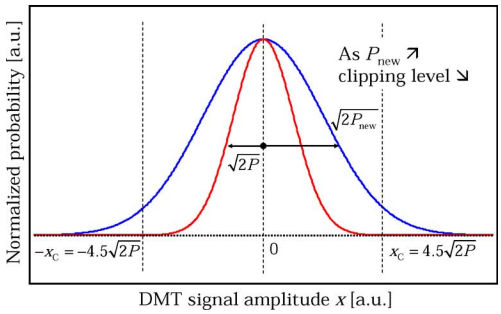

Fig. 4. Sketch of DMT waveform distribution and clipping. Clipping boundaries are kept constant (and scaled to the amplifier output), while the signal power is incrementally increased. Equivalently, clipping level is decreased. In each step, new loading algorithm result leads to higher throughput, but increased amount of clipping leads to higher error count. Signal power is increased until the acceptable BER limit is reached.

Subsequently, we tried to enhance the achievable transmission rate beyond 500 Mbit/s by allowing for more clipping. This was done in the following way. As illustrated in Fig. 4, depicting a sketch of a DMT waveform distribution in front of the amplifier (sketch of probability density function), the clipping limits of the digital signal were kept constant at $|x_{\mathrm{C}}| = 4.5\sqrt{2P}$, while the power of the unclipped signal was increased to $P_{\mathrm{new}} > P$ in steps of $\Delta P = P/10$. Equivalently, the clipping level was decreased in steps $\Delta \mathrm{CL} = |20 \log \sqrt{10/11}| \approx 0.4$ dB. As before, the clipped signal was then scaled to the same output range of the pre-amplifier (i.e., the modulation index of the LED remained unchanged).

In each step, i.e., for each new clipping level (new P_{new} value), we performed the loading algorithm resulting in a new bit- and power distribution. With these new distributions, we then conducted measurements as well as Monte Carlo simulations.

Clearly, as the amount of clipping grows (CL decreases), additional errors occur at the Rx decision unit. In each step, the loading algorithm was set to target a BER of $1 \cdot 10^{-3}$. When deriving the optimal loading mask, the algorithm takes into account only the errors due to noise at the receiver. So, by targeting "only" $1 \cdot 10^{-3}$ we allowed some margin in the design for the clipping induced errors before the BER limit of $2 \cdot 10^{-3}$ was reached. A target BER value of $1 \cdot 10^{-3}$ for bit-loading was chosen, since it is recommendable to design the system so that noise and clipping lead to the approximately same amount of errors [12], [13]. There, it was shown that in that way permitted controlled clipping is more advantageous than targeting the ultimate error performance limit with the loading algorithm $(2 \cdot 10^{-3})$ and not allowing for any clipping.

In Fig. 5 we show the results of our investigations, gained both from experiments and by means of simulations. The overall condition for investigations (both by measurements and simulations) was $\mathrm{BER}_{\mathrm{TOT}} \leq 2 \cdot 10^{-3}$ (given that such error rate can still be successfully handled by the FEC mechanism). In other words, a practical system and its somewhat idealized model were compared in terms of transmission rate performances under the same error rate constraint. Fig. 5(a) presents the obtained BERs as a function of the subcarrier index for

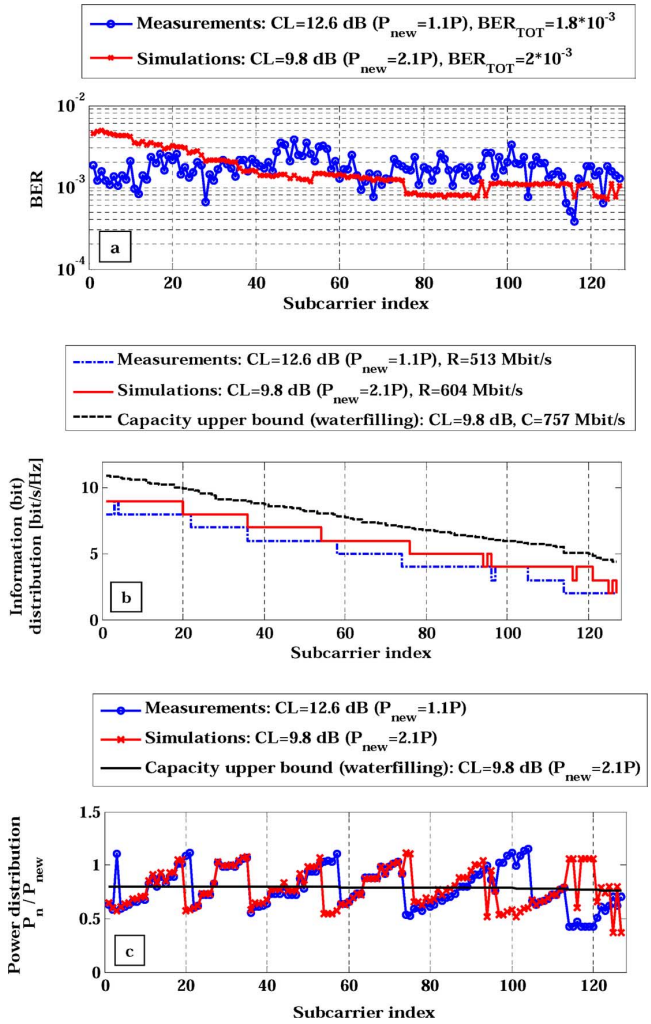

Fig. 5. Performance comparison of the experimental system (measurements) and its linear system model (simulations), under the condition $\mathrm{BER}_{\mathrm{TOT}} \leq 2 * 10^{-3}$. (a) BER values on individual subcarriers obtained by measurements and Monte Carlo simulations when clipping is permitted. (b) Optimal loading masks applied in measurements and simulations. (c) Optimal power distributions applied in measurements and simulations. The capacity upper bound is included in (b) and (c) as a theoretical benchmark.

maximum P_{new} (i.e., minimum clipping level CL) that results in $\mathrm{BER}_{\mathrm{TOT}} \leq 2 \cdot 10^{-3}$, whereas panels b and c show the corresponding bit-loading masks and power distributions. The results on the two latter panels present the output of the loading algorithm in case of measurements and simulations.

For measurements, only a minimal ~0.4 dB increase of the power was allowed (one ΔP step, or equivalently, clipping level decreased to CL $\approx$ 12.6 dB), for which $\mathrm{BER}_{\mathrm{TOT}}$ was still below the chosen acceptable limit. This small increase in signal power did however result in a (correspondingly small) rate improvement to 513 Mbit/s. In simulations, on the other hand, under the same error-performance condition, a much higher power increase of 3.2 dB was allowed (the clipping level decreased to CL $\approx$ 9.8 dB), leading to a significant improvement in throughput (604 Mbit/s). Fig. 6 shows how the simulated BER resultant increases with a decrease in the clipping level.

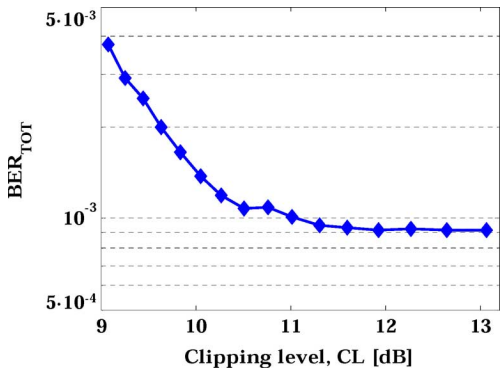

Fig. 6. Dependence of BER on the clipping level obtained by simulations.

The reason why clipping-level adaptation rendered only a marginal throughput enhancement in the measurements lies presumably in the fact that the performance of the regarded transmission system was limited by imperfect system linearity (primarily of the LED), rather than by clipping, [14]. Since the non-linearities are not taken into account by the simulations, this would also explain the large discrepancy (in terms of the allowed signal power, i.e., difference in clipping level, and as a consequence in the achievable rate) between the measurements and simulations results.[5] Moreover, calculation of the clipping percentage, obtained as the number of clipped samples over the total number of samples sent, was below 0.2% for simulations and negligible for measurements. In a perfectly linear system, one could permit much more clipping without pushing the BER over the limit, and in turn significantly increase the throughput. Hence, the loading mask shown for simulations in Fig. 5(b) can be regarded as an upper bound of the rate achievable in a practical not perfectly linear system.

Following approaches are imaginable towards further data rate increase in our link: (1) increasing the emitted optical dc power, (2) increasing the modulation index, and (3) compensating for the LED nonlinearities. Notice though, that in lighting applications the first approach is not an option, since the maximum illuminance is limited by illumination standards or user demands. Further, compensating electro-optical nonlinearities of the commercial LEDs used in VLC applications is not a trivial task, since their nonlinearity is frequency-dependent [15]. However, if one has access to a model describing these nonlinearities (gained, e.g., through a reverse-engineering approach as promoted in [16]), they can be suppressed on the receiver side by equalization [17] or through pre-distortion on the transmitter side [18], [19]. An overview on this topic was provided in [20].

Due to the lack of suitable low-impedance amplifiers (the differential impedance of the LED modules used is typically $\approx 3\ \Omega$ [21]), the modulation index was limited to $m = 0.16$ in our experiments. For considerations of a different m, σ^2 in noise-enhancement coefficients (in e.g., (2)) was replaced with $\sigma_m^2 = (m/0.16)^2\sigma^2$. Suppressing the interference caused by

[5]Note that since the algorithm has different signal powers P_{new} at its disposal for measurements and simulations, it is not expected that the resulting distributions of bits and powers in the two cases match to a high extent.

LED nonlinearity (e.g., in the receiver), and pushing the modulation index to $m = 1$ would increase the overall link budget by $20\log(1/0.16) \approx 16$ dB.[6] According to the simulations (which included bit- and power-loading plus clipping level adaption), this further enhanced the maximum achievable gross data rate to 1.14 Gbit/s (i.e., $\sim$1 Gbit/s net). It has to be noted, however, that the corresponding bit-loading mask involved modulation formats from 2^8-QAM to 2^{15}-QAM, which are high for a practical implementation.

As a further reference, we calculated the system capacity (assuming a perfectly linear system) by means of the well-known water-filling principle [22]. Water-filling relies on a Gaussian distribution of the signal at the channel input. Since we actually have a clipped Gaussian distribution in front of the optical source, when the same total power constraint is taken for water-filling, its result provides the upper capacity bound [12]. Nevertheless, having seen that the amount of clipping is quite small, the water-filling capacity bound can be considered as tight. It was, hereby assumed that the maximum signal power (i.e., clipping level 9.8 dB) in case of simulations is taken as the signal power limit for the water-filling algorithm. For this clipping level, results of the water-filling are included in Fig. 5(b) and (c), leading to the upper capacity bound of

$$C = \frac{B}{N}\sum_{n}\log_2\left(1+\frac{P_n}{\sigma^2/|H_n|^2}\right) \approx 757\,\text{Mbit/s}. \quad (4)$$

The water-filling algorithm renders the system capacity based on the Shannon limit, which allows an arbitrarily small (fractional) information quantity to be allotted to a subcarrier (whereas, in practical QAM-based systems, the smallest information quantity is a bit). This can be observed on the plots in Fig. 5(b). The value of 757 Mbit/s considered an LED modulation index of $m = 0.16$. For $m = 1$, the capacity bound would be at 1.74 Gbit/s.

IV. Summary and Conclusions

In this paper, we reported on a wireless point-to-point communication link based on a commercial white phosphorescent LED and an amplified APD. Within the BER margin of FEC $(2 \cdot 10^{-3})$ we demonstrated transmission at 513 Mbit/s gross data rate with off-line processing (450+ Mbit/s net, with 11% overhead deduction). This unprecedented high data rate was achieved by efficiently exploiting the bandwidth of the LED, due to a combination of DMT, multi-level modulation (QAM), bit- and power-loading, as well as symmetrical clipping.

The effectiveness of controlled clipping was found to be much lower than predicted by theory, and we believe that the nonlinear electro-optical characteristic of the LED is the reason for this. In an ideally linear system we project the highest achievable data rate to be over 600 Mbit/s for the conditions in our experiment.

[6]Such an increase of the modulation index could be achieved with better impedance matching and more powerful amplification. Multi-stage amplification is the traditional avenue toward higher amplification. We developed a prototype based on a two-stage amplifier approach. While our approach offers a much larger modulation index (0.7) it currently suffers from rather low modulation bandwidth of $\sim$13 MHz [21]. This is why we resorted to a larger-bandwidth commercial amplifier in this investigation.

Limiting factors in our experiment were the rather low modulation index (0.16) and presumably the LED nonlinearity. Assuming the same noise level in the receiver, our simulations predict that increasing the modulation index to 1, while compensating for the LED nonlinearities, would enhance the practically achievable (net) data rate to 1+ Gbit/s. The theoretical maximum throughput for such system (obtained by water-filling method) is 1.74 Gbit/s.

Acknowledgment

The authors thank S. Randel, Siemens AG, now with Alcatel-Lucent Bell Labs, USA for valuable comments on the paper.

References

[1] D. O'Brien *et al., Short-Range Wireless Communications*, M. Kreamer and M. D. Katz, Eds. New York: Wiley, 2009.
[2] K.-D. Langer *et al.*, "Advances and prospects in high-speed information broadcast using phosphorescent white-light LEDs," in *Proc. ICTON*, 2009, p. Paper Mo.B5.3.
[3] J. Vucic *et al.*, "White light wireless transmission at 200+ Mbit/s net data rate by use of discrete-multitone modulation," *IEEE Photon. Technol. Lett.*, vol. 21, no. 20, pp. 1511–1513, Oct. 2009.
[4] J. Vucic *et al.*, "230 Mbit/s via a wireless visible-light link based on OOK modulation of phosphorescent white LEDs," in *Proc. OFC/NFOEC*, 2010, Paper OThH3.
[5] J. Grubor, S. C. J. Lee, K. D. Langer, T. Koonen, and J. W. Walewski, "Wireless high-speed data transmission with phosphorescent white-light LEDs," in *Proc. ECOC*, 2007, Paper PD3.6.
[6] *Lighting of Indoor Work Places*, European Standard EN 12464-1, 2003.
[7] J. Vucic, C. Kottke, S. Nerreter, K. Habel, A. Buettner, K.-D. Langer, and J. W. Walewski, "125 Mbit/s over 5 m wireless distance by use of OOK-modulated phosphorescent white LEDs," in *Proc. ECOC*, 2009, Paper 9.6.4.
[8] A. Goldsmith, *Wireless Communications*. Cambridge, U.K.: Cambridge Univ. Press, 2005.
[9] B. S. Krongold, K. Ramchandran, and D. L. Jones, "Computationally efficient optimal power allocation algorithms for multicarrier communication systems," *IEEE Trans. Commun.*, vol. 48, no. 1, pp. 23–27, Jan. 2000.
[10] F. Xiong, *Digital Modulation Techniques*, 2nd ed. Norwood, MA: Artech House, 2006.
[11] ITU-T Recommendation G.975.1 (02/2004).
[12] J. Vucic, "Adaptive modulation technique for broadband communication in indoor optical wireless systems," Ph.D. dissertation, Technische Universitaet, Berlin, Germany, 2009.
[13] J. Grubor and K.-D. Langer, "Efficient signal processing in OFDM-based indoor optical wireless links," *J. Netw.*, vol. 5, no. 2, pp. 197–211, Feb. 2010.
[14] B. Inan *et al.*, "Impact of LED nonlinearity on discrete multitone modulation," *J. Opt. Commun. Netw.*, vol. 1, pp. 439–451, 2009.
[15] S. Camatel *et al.*, "LED non-linearity characterization and compensation," in *Proc. ICPOF*, 2007.
[16] T. Kamalakis, J. W. Walewski, G. Ntogari, and G. Mileounis, *Empirical Volterra-Kernel Modeling of Commercial Light-Emitting Diodes*, 2010, to be published.
[17] L. Agarossi, S. Bellini, F. Bregoli, and P. Migliorati, "Equalization of non-linear optical channels," in *Proc. ICC*, 1988, vol. 2, pp. 662–667.
[18] A. Brajal and A. Chouly, "Compensation of nonlinear distortions for orthogonal multi-carrier schemes using predistortion," in *Proc. GLOBECOM*, 1994, vol. 3, pp. 1909–1914.
[19] M. C. Kim, Y. Shin, and S. Im, "Compensation of nonlinear distortion using a predistorter based on the fixed point approach in OFDM systems," in *Proc. VTC*, 1998, pp. 2145–2149.
[20] E. Biglieri, S. Barberis, and M. Catena, "Analysis and compensation of nonlinearities in digital transmission systems," *IEEE J. Sel. Areas Commun,*, vol. 6, no. 1, pp. 42–51, Jan. 1988.
[21] R. Baumgartner, A. Kornbichler, and J. Walewski, "High-power high-bandwidth linear driving circuit for VLC applications," *Working Group IEEE 802.15*.
[22] T. M. Cover and J. A. Thomas, *Elements of Information Theory*. New York: Wiley, 1991.

Jelena Vučić received the Diploma in electrical engineering with emphasis on Telecommunications, at Belgrade University, Belgrade, in 2002 and the Ph.D. degree in 2009 at Technische Universitaet Berlin, Germany.

In 2003, she joined the Fraunhofer Institute for Telecommunications, Heinrich-Hertz-Institut, in Berlin, Germany, where she works as a research assistant in the Department of Photonic Networks and Systems. The main topic of her thesis was the investigation of advanced signal processing techniques in broadband optical wireless systems. Her current research interests include optical access and indoor networks and optical wireless systems.

Christoph Kottke is a student of electrical engineering at the Technische Universitaet Berlin, Germany.

He works as a student research assistant in the Department of Photonic Networks and Systems at the Fraunhofer Institute for Telecommunications, Heinrich-Hertz-Institut (HHI) Berlin. Currently, he is fishing his diploma thesis in the area of optical wireless communications.

Stefan Nerreter received the technical diploma in telecommunication from Technical College Burg in 1989 and the engineering diploma in physical sciences at Technische Hochschule Wildau, Germany, in 2000.

Between 2000 and 2001 was with the Max-Born-Institute and worked on the development of a scanning microscope for the inspection of high-power laser diodes. From 2001 to 2004 he worked with Infineon Fiber Optics as an engineer for failure analysis of electro-optical components. Since 2004, he has been with Siemens Corporate Technology. As a Senior Engineer in the area of Optic in Electronic Assemblies and Interconnects in the department of Materials and Microsystems he supports customer R&D projects and has been involved in several funded R&D projects.

Klaus-Dieter Langer graduated from tje Braunschweig-Wolfenbuettel University of Applied Sciences and received the diploma degree in electrical engineering from the Technische Universitaet Berlin, Germany.

In 1981, he joined Heinrich-Hertz-Institut (HHI), Berlin, as a research associate working on broadband communications. He has been involved in numerous research projects where he has worked mainly on the design and performance evaluation of photonic switching systems and networks. In 1992, he joined the German Federal Ministry of Research and Technology where he served as an adviser on national telecommunications, digital audio broadcasting, and photonics/optoelectronics R&D. At HHI, he subsequently addressed the use of optical and photonic technologies in communication networks, their layout and, in particular, the topic of cost-efficient optical subscriber lines and the use of WDM for optical access. He is currently in charge of research on optical access and indoor networks at the Photonic Networks and Systems Department of the Fraunhofer Institute for Telecommunications, HHI.

Joachim W. Walewski received the diploma degree in physics (Dipl.-Phys) in 1995 from the Christian Albrechts University, Germany, and the Ph.D. degree from the Lund Institute of Technology, Sweden, in 2002, for his research in applied laser spectroscopy.

After stints at the Tampere University of Technology, Finland, the Lund Institute of Technology, and the Engine Research Center of the University of Wisconsin—Madison, U.S.A., he joined Siemens Corporate Technology in Munich, Germany in 2006. There, his efforts have focused on R&D in the fields of wireless optical communications, Green ICT, and the Internet of Things.